Energetics of Charged Particle-Induced Fission Reactions*

H. C. Britt, H. E. Wegner,† and Judith C. Gursky

Los Alamos Scientific Laboratory, University of California, Los Alamos, New Mexico

(Received 8 October 1962)

Measurements with a semiconductor detector system and a two-dimensional analyzer have yielded information on the mass distributions and the details of the kinetic energy release from a series of charged particle-induced fission reactions. The fissioning compound nuclei range from thallium for which the mass distributions are symmetric, to plutonium for which the fission is predominantly asymmetric. In an intermediate region, the charged particle-induced fission of Ra^{226} yields comparable contributions of symmetric and asymmetric fission. All of the results are quantitatively consistent with a two-mode hypothesis for the fission process and indicate that within each mode the distance between the charge centers of the two fragments at the scission point is approximately the same for all mass divisions. The results show a lower total kinetic energy release from symmetric fission than from asymmetric fission, indicating that the distance between the charge centers at the scission point is about 10% greater for the symmetric mode than for the asymmetric mode.

1. INTRODUCTION

ONE of the more interesting problems in the study of the fission process has been the understanding of the existence of the two types of mass distributions, symmetric and asymmetric, and the competition between them. Measurements of fission mass and energy distributions have been made by a large number of experimenters for many different fissioning nuclei over a large range of excitation energies. Reference to most of this work can be found in recent review articles.[1-3]

Early measurements on the fission of thorium and heavier elements showed that their mass distributions were predominantly asymmetric, and the peak-to-valley ratios of the mass distributions decreased markedly with increasing excitation energy. This observation prompted Turkevich and Niday[4] to suggest that the increase in the symmetric yield could be due to a symmetric fission mode which became more probable as the excitation energy of the compound nucleus increased. Such an interpretation became more plausible with the radiochemical work of Fairhall et al.,[5-7] which showed that fission was predominantly symmetric for compound nuclei of polonium and lighter elements, and both symmetric and asymmetric fission competed with approximately equal probability in a transition region at radium and actinium. In this region the symmetric mode was also observed to increase very rapidly relative

to the asymmetric mode as the excitation energy increased.

In addition to the radiochemical measurements, there have been experiments in which the total kinetic energy releases in fission were determined by measuring either the velocities, energies, or ranges of the two fragments.[1-3] These measurements have all been for the fission of thorium and heavier elements, for which statistics and resolution are inadequate to give significant information on the total kinetic energy releases from the highly improbable symmetric fission for most of the cases studied. However, for the thermal-neutron-induced fission of U^{233}, U^{235}, and Pu^{239}, it was shown that the average total kinetic energy release from symmetric fission was approximately 30 MeV less than that from the asymmetric fission mode.[8-10] Measurements have also been made by Whetstone and Leachman[11] on He^4-induced fission of Th^{232} and U^{233}, which give relative symmetric yields that are an order of magnitude greater than those for the thermal neutron cases. Their results also show a decrease in the total kinetic energy release from symmetric fission, but in this case the decrease was only 10–15 MeV.

One possible interpretation of these data, which has been suggested by Niday,[10] is that the symmetric fission arises from a true symmetric mode and that the total kinetic energy release in the symmetric mode is less than that in the asymmetric mode. The purpose of this experiment is to investigate this hypothesis and study the competition between symmetric and asymmetric fission.

In this experiment, various fissioning nuclei were formed with moderate excitation energies (10–30 MeV) by charged-particle bombardment. These nuclei cover a Z^2/A range from nuclei where the fission is almost

[1] I. Halpern, Ann. Rev. Nuc. Sci. 9, 245 (1959).
[2] E. K. Hyde, University of California Radiation Laboratory Reports, UCRL-9036 and UCRL-9065, 1960 (unpublished).
[3] J. R. Huizenga and R. Vandenbosch, in *Nuclear Reactions, Vol. II*, edited by P. M. Endt and M. Demenr (North-Holland Publishing Company, Amsterdam, to be published).
[4] A. Turkevich and J. B. Niday, Phys. Rev. 84, 52 (1951).
[5] A. W. Fairhall, Phys. Rev. 102, 1335 (1956).
[6] R. C. Jensen and A. W. Fairhall, Phys. Rev. 109, 942 (1958); 118, 771 (1960).
[7] A. W. Fairhall, R. C. Jensen, and E. F. Neuzil, in *Proceedings of the Second International Conference on the Peaceful Uses of Atomic Energy, Geneva, 1958* (United Nations, Geneva, 1958), Vol. 15, p. 452.

[8] J. C. D. Milton and J. S. Fraser, Phys. Rev. Letters 7, 67 (1961).
[9] W. M. Gibson, T. D. Thomas, and G. L. Miller, Phys. Rev. Letters 7, 67 (1961).
[10] J. B. Niday, Phys. Rev. 121, 1471 (1961).
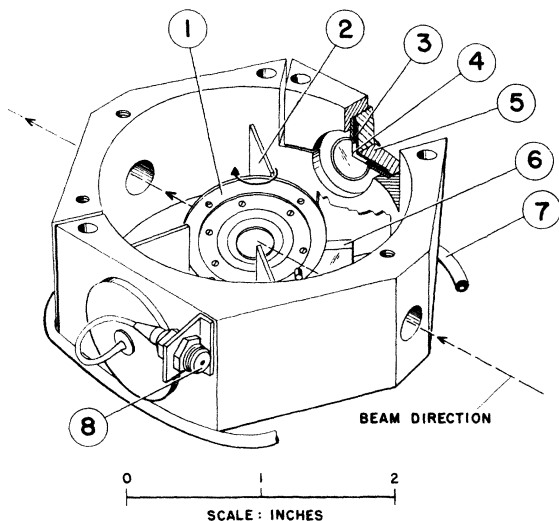[11] S. L. Whetstone and R. B. Leachman, Bull. Am. Phys. Soc. 6, 376 (1961).

FIG. 1. The detector-target holder. (1) Target holder. (2) Baffle for shielding detectors from collimator-scattered beam particles. (3) Gold-defining aperture. (4) Nickel absorber foils (50 μg/cm^2). (5) Gold-surface barrier detector. (6) Insulated Lucite target holder support. (7) Water cooling lines. (8) Miniature coaxial cable connector for signal.

entirely symmetric to nuclei where asymmetric fission is predominant. The symmetric fission reactions studied were He^3-induced fission of Au^{197}, Tl^{203}, Tl^{205}, Pb^{206}, and Bi^{209}. The study of the intermediate region consisted of an investigation of the fission of Ra^{226} induced by deuterons, He^3, and He^4 particles at various bombarding energies. The predominantly asymmetric fission reactions were proton-induced fission of Th^{230} and He^4-induced fission of U^{233}. From the investigation of the predominantly symmetric and asymmetric reactions, it was possible to determine the general properties of the kinetic energy release from fission that is either predominantly symmetric or asymmetric. The study of the intermediate region then resulted in information concerning the competition between symmetric and asymmetric fission. A preliminary report of some of these results has been previously published.[12]

2. EXPERIMENTAL PROCEDURE

It was advantageous to detect fission fragments with as large a solid angle as possible, because of the small fission cross sections (<1 mb) for the symmetric fission reactions. Consequently, the energies of the two coincident fragments were measured with two 300 Ω-cm gold-surface barrier semiconductor detectors,[13] subtending solid angles of approximately 1%. A sketch of the apparatus is shown in Fig. 1. The two gold-surface barrier semiconductor detectors were placed in a back-to back arrangement at an angle of 90° relative to the beam direction. They were approximately 1.5 in. from

[12] H. C. Britt, H. E. Wegner, and J. Gursky, Phys. Rev. Letters 8, 98 (1962).

[13] The semiconductor detectors were obtained from Oak Ridge Technical Measurements Corporation, Oak Ridge, Tennessee.

the target and had a detection area that was defined by a $\frac{1}{2}$-in.-diam gold collimator. These collimators restricted the detection area so that particles would not be detected near the edges of the sensitive area of the detector. The detectors were clamped in a brass holder, and at large beam currents (~ 1 μA) water cooling of this holder was necessary to maintain constant detector currents. The targets were mounted at a 45° angle relative to the charged particle beam direction, and provision was made for rotating the target through an angle of 180°, so that the energy loss from fragments traversing the target backing could be determined. The target was mounted on a Lucite holder allowing the application of a bias voltage that was found necessary because of background problems which are discussed below.

Accelerated charged particle beams from the Los Alamos variable energy cyclotron were collimated to a $\frac{1}{4}$-in.-diam circle on the center of the target. After traversing the detector-target chamber (Fig. 1), the beam was collected in a Faraday cup, and the integrated beam was monitored with a current integrator. Baffles were placed around the detectors so that only particles from the target could be detected. The detector-target chamber was mounted in a vacuum system that was connected to the cyclotron for all measurements except those of radium for which the vacuum system was isolated from the cyclotron by a 0.4-mil Mo window in order to prevent radon contamination of the cyclotron. The variation in the average beam energy during the period of a typical set of measurements (~ 1 day) was approximately ± 0.2 MeV.

All of the targets except radium were prepared by evaporation on nickel backings of approximately 100-μg/cm^2 areal density. The Au^{197}, Tl, Pb^{206}, and Bi^{209} targets had areal densities of 100–200 μg/cm^2, which were determined to an accuracy of $\pm 20\%$ by measuring the elastic scattering for 25.5-MeV He^3 ions at 90° and comparing with other measurements.[14] The Au^{197} and Bi^{209} targets were monoisotopes. The Pb^{206} target had an isotopic composition of 88% Pb^{206}, 9% Pb^{207}, and 3% Pb^{208}. The Tl target contained the natural isotopic mixture of Tl^{203} and Tl^{205}. The Th^{230} and U^{233} targets had areal densities of 20–30 μg/cm^2, which were determined from the alpha activity of the target and the area of the deposit. The Th^{230} target had an isotopic composition of 90.2% Th^{230} and 9.8% Th^{232} and the U^{233} target was 99% monoisotopic. The Ra^{226} target was made by electrospraying and contained 32 μg of Ra^{226} on an area of approximately 1 cm^2.

The semiconductor detectors were operated at a bias of 70 V. At this bias voltage, the depletion depth was thicker than the range of the most energetic fission fragment or calibration alpha particle but thin enough that elastically-scattered He^3 and alpha particles from the cyclotron lost only 2–3 MeV in the counters.

[14] D. D. Armstrong, Master's thesis, University of New Mexico (1961).

The signals from the two detectors were analyzed in a two-dimensional analyzer, consisting of two 200-channel analog-to-digital converters with a read-out system that recorded the two coincident pulse heights on punched paper tape. The data recorded on the paper tapes were then sorted and processed in a digital computer.[15] The two-dimensional analyzer was gated by a coincidence between the two fission detectors, so that only events corresponding to the detection of both fragments were recorded. The singles fragment spectra from the two detectors were also monitored in a 400-channel pulse-height analyzer.

The gain of the electronic system of each detector was checked approximately once an hour by measuring the pulse heights for known energy alpha-particle groups. These alpha-particle spectra were recorded in a 400-channel analyzer, and positions of the peaks were determined with a Gaussian-fitting computer code.[16] For a typical measuring period of 2–3 weeks, the over-all drift or instability of the system (detectors plus amplifiers) was $\lesssim 1\%$. Since small long term drifts could be partially corrected with the alpha-particle calibrations, the over-all stability of the system was better than 0.5%.

In the Bi, Pb, Tl, and Au experiments beam currents of 0.5–1.0 μA were found to strongly affect the detector resolutions because of the electronic pile up caused by low-energy negatively charged particles from the target. These particles were eliminated by an 800-μg/cm² Al absorber in front of the detector; however, this thickness could not be used when measuring fission fragments. The resolution could also be improved by a factor of $\sim$3 with a 2-kV positive bias on the target. For the Bi, Pb, Tl, and Au reactions, the data were taken with 50-μg/cm² Ni absorbers in front of the detectors and a 2-kV positive bias on the target. This combination resulted in a tenfold improvement in the resolution. In all cases the beam currents were kept at a level such that the electronic noise contribution to the resolution for fission fragments was 3–4%. This resolution introduced a dispersion into the data that was approximately the same as the dispersion due to neutron effects. In the Ra²²⁶ and heavier element experiments, the fission cross sections were much higher, so that small beam currents (<0.1 μA) were used, and the Ni absorber foils and target bias were not needed.

3. METHOD OF CALIBRATION AND DATA ANALYSIS

A. Energy Calibration

The energy calibration of the two fission channels was obtained with a Cf²⁵² spontaneous fission source, several known energy alpha-particle groups, and a precision mercury-switch pulser. The zero channel positions of

the two analog-to-digital converters and the required amplifier gain change between fission-fragment and alpha-particle measurements were determined with the pulser. The slope of the fragment energy to pulse-height relationship was determined by measuring the pulse heights for several known energy alpha particle groups. In both of these measurements the peak pulse-height positions could be determined to better than 0.1% with the previously mentioned fitting code.[16] The Cf²⁵² spontaneous fission source was used to determine the pulse-height defects for the two detectors and the energy loss for the fragments in the 50-μg/cm² Ni absorbers in front of the detectors, by a comparison between the observed pulse heights for the two Cf²⁵² energy groups and the time-of-flight results of Milton and Fraser.[17] In this comparison the energies used were the values estimated for the final energies of the two Cf²⁵² energy groups.[18] The sum of the pulse-height defect and the energy loss in the absorber foils was found to be the same for the two Cf²⁵² energy groups and for the two detectors to within ±0.5 MeV.[19]

In the analysis of the data, the pulse-height defects and energy degradation in the target deposit, Ni target backings, and Ni-detector cover foils were assumed to be the same for all fission fragments. The energy loss in the target backing foil was determined from data taken in each of two orientations with the target at 45° and 225° with respect to the beam direction. The average energy loss in the target material was obtained from the range-energy relations of Alexander and Gazdik.[20] These target-thickness corrections were significant only for the Au, Tl, Pb, and Bi targets.

The calibration procedure yielded kinetic energies for the fragments that were accurate to ±1% relative to the results reported by Milton and Fraser.[17]

B. Method of Data Analysis

The data obtained from the two-dimensional analyzer were sorted and the results compiled in a computer. The data analysis for each event consisted of converting the two pulse heights to energies and then calculating the two masses by assuming the ratio of the two initial masses to be equal to the ratio of the two measured energies. It was necessary to smooth the pulse-height distributions in order to avoid obtaining spurious structure in the mass and energy distributions due to the finite size of the pulse-height channels. This smoothing was done by

[15] IBM 7090 computers were used to process all of the data presented herein.
[16] P. McWilliams, W. S. Hall, and H. E. Wegner, Rev. Sci. Instr. 33, 70 (1962).

[17] J. C. D. Milton and J. S. Fraser, Phys. Rev. 111, 877 (1958).
[18] These final energies were determined by fitting the reported initial energy distributions (see reference 17) with the same fitting code that was used in treating the data. Then from the peak energy values the average change due to the isotropic emission of 1.9 neutrons/fragment was subtracted yielding final peak energies for the two Cf²⁵² energy groups of 102.2 and 78.4 MeV.
[19] A more complete discussion of pulse-height defects and of the effects of neutron emission will be given by H. C. Britt, and H. E. Wegner, Rev. Sci. Intr. (to be published) and H. C. Britt, H. E. Wegner, and S. L. Whetstone (to be published).
[20] J. M. Alexander and M. F. Gazdik, Phys. Rev. 120, 874 (1960).

adding a random number between $-\frac{1}{2}$ and $+\frac{1}{2}$ to each pulse height. For a given set of data, the events were sorted to give the energy and mass spectra in each of the two channels, the total kinetic energy release spectrum, and a probability matrix for the total kinetic energy release versus the mass ratio of the two fragments. The average value of the final total kinetic energy release, $\bar{E}_{Kf}$, and a value for the variance, $\sigma^2(E_K) = \langle E_{Kf}^2 \rangle_{\rm av} - \bar{E}_{Kf}^2$ were computed for each mass ratio group.

C. Effects Due to Neutron Emission from the Fragment

The fragment energies measured in this experiment represent the final energies after the emission of some average number of neutrons. However, to obtain information about the fission process, it is advantageous to determine the initial total kinetic energy releases. If it is assumed that an average number of neutrons, $\bar{\nu}$, are emitted isotropically and in equal numbers from the fully accelerated fragments, then for a given fission mass ratio $(R = m_H/m_L)$, the average initial total kinetic energy release, $\bar{E}_K$, is related to the average final total kinetic energy release, $\bar{E}_{Kf}$, by

$$\bar{E}_K = \bar{E}_{Kf} + \Delta E, \tag{1}$$

where

$$\Delta E \cong \frac{\bar{\nu}}{2(m_{Hf} + m_{Lf})} \bar{E}_{Kf} \frac{R^2 + 1}{R}, \tag{2}$$

and m_H and m_L are the initial heavy and light fragment masses, and m_{Hf} and m_{Lf} are the final heavy and light fragment masses.

The major difficulty encountered in applying this correction to the data is that to the present time there have been no measurements of $\bar{\nu}$ for any of the reactions studied. However, it is possible to estimate $\bar{\nu}$ from calculated fission energy releases and neutron binding energies[21] in the following way. First, the average excitation energy, E^*, for the two fragments is estimated from the total energy release and the total kinetic energy release. This excitation energy is then considered dissipated in the emission of neutrons and γ rays. The average total energy of the γ rays is assumed to be the same in all cases and is taken equal to 7.5 MeV.[8,17] It is then assumed that the average number of neutrons from each fragment was the same and that their average kinetic energy is 1.2 MeV, then $\bar{\nu}$ can be obtained from the excitation energy available for neutron emission, E_n^*, by

$$\bar{\nu} = E_n^*/(\bar{B}_n + 1.2), \tag{3}$$

where $\bar{B}_n$ is the average neutron binding energy in the two fragments. This method for estimating $\bar{\nu}$ is approximate; however, for the reactions studied ΔE is 1–3% of $\bar{E}_K$ so that an uncertainty of 20% in ΔE results in an

[21] J. C. D. Milton, University of California Radiation Laboratory Report, UCRL-9883 Rev., 1962, and (private communication).
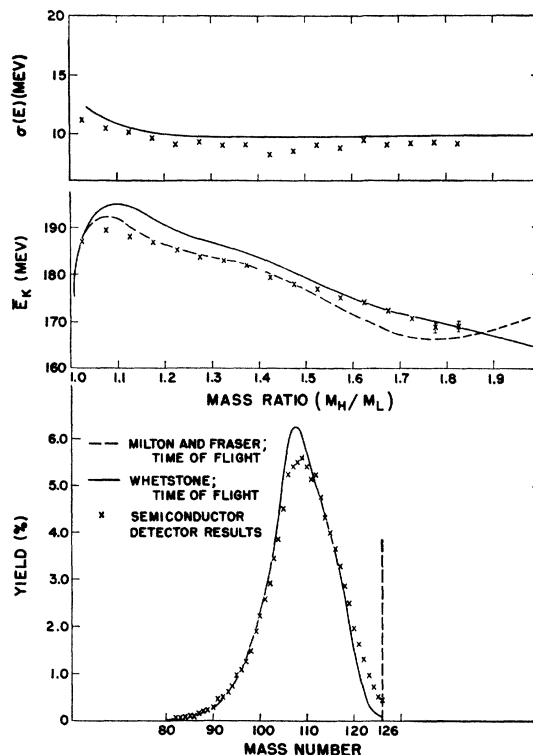
FIG. 2. A comparison of the results obtained with the semiconductor detector system to the time-of-flight results of Whetstone and Milton and Fraser for the spontaneous fission of Cf^{252}.

uncertainty in $\bar{E}_K$ of 0.2–0.6%, which is approximately the same as the experimental uncertainties in the energy calibration.

In addition to this small decrease in the fragment energies, the emission of neutrons from the fragments also introduces a dispersion into the results. Terrell[22] has shown that this dispersion comes from two factors. For direct energy measurements, the dispersion due to isotropic emission of neutrons from the two fragments gives a mass resolution function with a variance, $\sigma^2(m)$, that is four times the variance for time-of-flight measurements. However, in the direct energy measurements an additional dispersion is present if the number of neutrons from each fragment is not the same, as has been found[23,24] for spontaneous fission of Cf^{252} and thermal-neutron-induced fission of U^{233}. This dispersion not only tends to broaden the mass distribution but also distorts it slightly. For spontaneous fission of Cf^{252} and thermal-neutron-induced fission, the dispersion due to the emission of unequal numbers of neutrons from the two fragments is larger than that calculated for equal isotropic emission. Therefore, since no information is available on the details of neutron emission for the reactions being studied, it was not possible to make any

[22] J. Terrell, Phys. Rev. 127, 880 (1962).
[23] S. L. Whetstone, Jr., Phys. Rev. 114, 581 (1959).
[24] J. S. Fraser and J. C. D. Milton, Phys. Rev. 93, 818 (1954).

TABLE I. Characteristics of the energy and mass distributions for the fission reactions studied. E_{lab} and E^* are the laboratory bombarding energy and the excitation energy of the compound nucleus, respectively. $\langle \bar{E}_{Kf} \rangle$ and $\langle \bar{E}_K \rangle$ are, respectively, the average final and initial total kinetic energy releases for all mass divisions and $\sigma^2(E_K)$ is variance of these distributions. $\sigma_a^2(m)$ and $\sigma_s^2(m)$ are the variances of the asymmetric and symmetric mass peaks, respectively. $(Y_s/Y_T)_1$ and $(Y_s/Y_T)_2$ are the relative symmetric yields obtained from an analysis of the mass ratio distributions discussed in the text and from a least-squares fit of the mass distribution to a sum of three Gaussians, respectively.

Target	Projectile	E_{lab} (MeV)	E^* (MeV)	$\langle \bar{E}_{Kf} \rangle$ (MeV)	$\langle \bar{E}_K \rangle$ (MeV)	$\sigma^2(\bar{E}_K)$ (MeV)²	$\bar{m}_L$ (amu)	$\sigma_a^2(m)$ (amu)²	$\sigma_s^2(m)$ (amu)²	$(Y_s/Y_T)_1$	$(Y_s/Y_T)_2$
Au197	He3	25.5	35.9	138.6±2	140.3	55±3	...	...	96.7±3	1.0	1.0
Tl^nat	He3	25.5	35.6	139.0±2	141.7	50±3	...	...	89.0±3	1.0	1.0
Pb206	He3	25.5	33.0	143.6±2	145.4	50±3	...	...	79.1±3	1.0	1.0
Bi209	He3	25.5	30.6	145.4±2	147.3	57±3	...	...	85.0±3	1.0	1.0
		22.1	27.2	144.8±2	146.5	48±3	...	...	72.7±3	1.0	1.0
Ra226	d	14.0	21.8	150.9±2	154.9	88±5	89.8±0.3[a]	47.0±5[a]	100.0±10[a]	0.59	0.58
		11.7	19.5	151.0±2	154.9	90±5	89.5±0.3[a]	43.5±5[a]	90.0±10[a]	0.53	0.51
		9.8	17.6	152.0±2	155.8	89±5	88.9±0.3[a]	38.5±5[a]	96.0±10[a]	0.44	0.43
Ra226	He4	27.1	22.1	156.8±2	160.3	88±5	89.9±0.4[a]	38.0±2[a]	160.0±40[a]	0.24	0.30
		22.1	17.1	156.8±2	159.7	83±5	90.0±0.4[a]	38.5±2[a]	140.0±40[a]	0.16	0.19
Ra226	He3	23.4	32.2	154.4±2	158.9	94±5	90.1±0.6[a]	47.5±5[a]	130.0±20[a]	0.52	0.60
		20.9	29.7	153.4±2	157.7	93±5	89.6±0.6[a]	44.0±5[a]	160.0±30[a]	0.51	0.60
Th230	p	8.0	12.8	159.6±2	162.6	92±5	93.3±0.3[a]	48.5±2[a]	...	0.14	0.09
		6.8	11.6	159.4±2	162.4	90±5	92.8±0.3[a]	45.0±2[a]	...	0.09	0.06
U233	He4	25.5	19.9	165.8±2	170.3	117±6	b	b	b	<0.25	b
Cf252	Spont	...	...	179.4±2	182.9	106±6	108.9±0.3	55.4±2	...	...	...

[a] These values have been obtained from a least-squares fit of the mass distribution to a sum of three Gaussian distributions and are, therefore, dependent on the validity of the assumption of a Gaussian shape for the symmetric and asymmetric peaks.
[b] The Gaussian fitting technique used in the analysis of the Ra226 and Th230 results did not give a reasonable fit to this mass distribution.

meaningful resolution corrections to the results presented here. However, all of the conclusions that will be made are of a general nature and will not be affected by the experimental mass resolution.

D. Comparison with Time-of-Flight Results

Because of the difficulty in estimating the effects of neutron dispersion on these results, two comparisons were made between results taken with this semiconductor detector system and time-of-flight measurements.[17,25] These comparisons were made for the spontaneous fission of Cf252, for which the details of the neutron emission are known,[23] and 25.5-MeV He4-induced fission of U233, which represents a moderate excitation energy reaction more analogous to the ones being studied here.

The comparison for Cf252 is shown in Fig. 2. The mass distribution obtained with the semiconductor detectors indicates a mass resolution that is slightly poorer than that for the time-of-flight results, and there is a noticeable shift in the average mass for the two sets of results. The most important factor contributing to this shift is the dispersion due to the unequal numbers of neutrons from the two fragments.[19,22] The semiconductor detector results indicate a measured variance for the mass peak of $\sigma^2(m) = 55.4 \pm 2$ which can be compared to an intrinsic value of $\sigma^2(m) = 47.6 \pm 4$.[22] These results indicate a dispersion in the measured mass distribution of $\sigma^2(m) = 8.8 \pm 6$ which agrees with Terrell's estimate[22] of the dispersion due to the neutron emission effects discussed previously. This dispersion corresponds to a full width at half maximum for a Gaussian resolution function of $\Delta m = 6.5 \pm 2.5$ mass units which can be compared

[25] S. L. Whetstone, Jr. (private communication).

to the estimated neutron dispersion in time-of-flight measurements of $\Delta m = 2.2$ mass units.[25] The fact that the observed dispersion can be accounted for by neutron effects alone indicates that the dispersion due to neutron emission effects is large compared to any experimental dispersion that may be present due to detector resolutions, calibration uncertainties, etc.

The comparison of the dependence of the average total kinetic energy on mass ratio shows a shift that is within the uncertainties of the absolute energies and also shows a difference in the slope at large mass ratios as indicated in Fig. 2. This difference in slope can be attributed in part to the fact that the semiconductor detector results have not been corrected for mass dispersion and possibly also due in part to uncertainties in the slope of the energy calibration. It is reasonable to expect that similar uncertainties would be present in
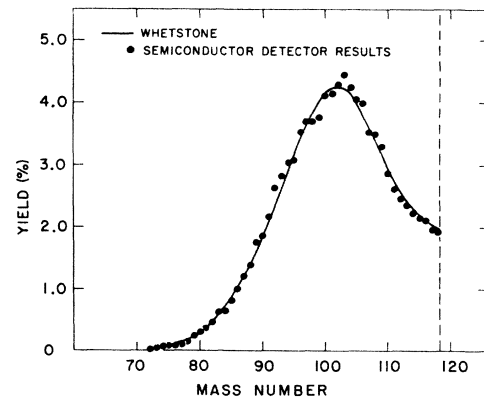

FIG. 3. A comparison of the results obtained with the semiconductor detector system to the time-of-flight results of Whetstone for the 25.5-MeV He4-induced fission of U233.

the other experimental results at large mass ratios. The dependence of the standard deviation for the total kinetic energy distributions, $\sigma(E)$, on mass ratio is very similar to the time-of-flight results.

The results obtained for 25.5-MeV He[4]-induced fission of U[233] are shown in Fig. 3. In this case, the mass spectra are indentical to within the statistical uncertainties, indicating approximately equal mass resolutions for the two experiments. For the time-of-flight results the mass resolution function was estimated by Whetstone[25] to have a $\Delta m \cong 3$ mass units which corresponded to approximately equal contributions from neutron effects and from instrumental dispersions. For the semiconductor detector results the total dispersion that is expected from isotropic emission of an equal number of neutrons from each fragment predicts $\Delta m \cong 4$ mass units.[22] Since the dispersion in the semiconductor results in this case seems to be somewhat less than that for the Cf[252] case and the mass distribution does not show the shift observed in the Cf[252] comparison, the number of neutrons from the fragments may not be as unequal as for Cf[252].

4. EXPERIMENTAL RESULTS

The reactions which were studied in this experiment and some of the characteristics of the energy and mass distributions which were obtained are listed in Table I. For the 25.5-MeV He[3]-induced fission of Bi[209], 160 000 events were recorded. For all of the other reactions studied, the results are based on a total of 20 000–30 000 events.
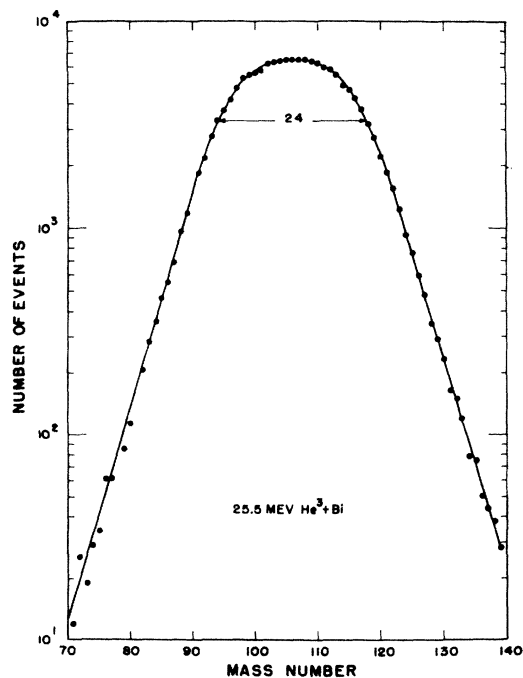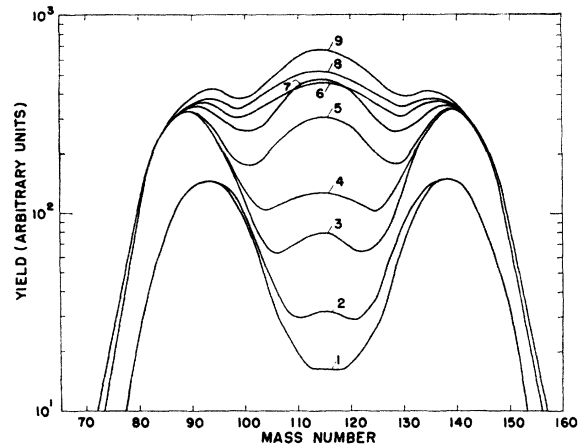

FIG. 5. A composite mass distribution for the asymmetric fission reactions studied. Each curve represents the best fit by eye to data with statistical uncertainties similar to the results presented in Figs. 2 and 3. The distributions have been arbitrarily normalized vertically and the mass number scale has been shifted by 0.5 mass unit for the He[4]+Ra[226] and d+Ra[226] results, so that all of the Ra[226] results are symmetric about mass number 114.5. The labels on the curves refer to the following fission reactions with excitation energies, E^*, for the compound nucleus: (1) 6.8-MeV p+Th[230], E^*=11.6 MeV; (2) 8.0-MeV p+Th[230], E^*=12.8 MeV; (3) 22.1-MeV He[4]+Ra[226], E^*=17.1 MeV; (4) 27.1-MeV He[4]+Ra[226], E^*=22.1 MeV; (5) 9.8-MeV d+Ra[226], E^*=17.6 MeV; (6) 20.9-MeV He[3]+Ra[226], E^*=29.7 MeV; (7) 11.7-MeV d+Ra[226], E^*=19.5 MeV; (8) 23.4-MeV He[3]+Ra[226], E^*=32.2 MeV; (9) 14.0-MeV d+Ra[226], E^*=21.8 MeV.

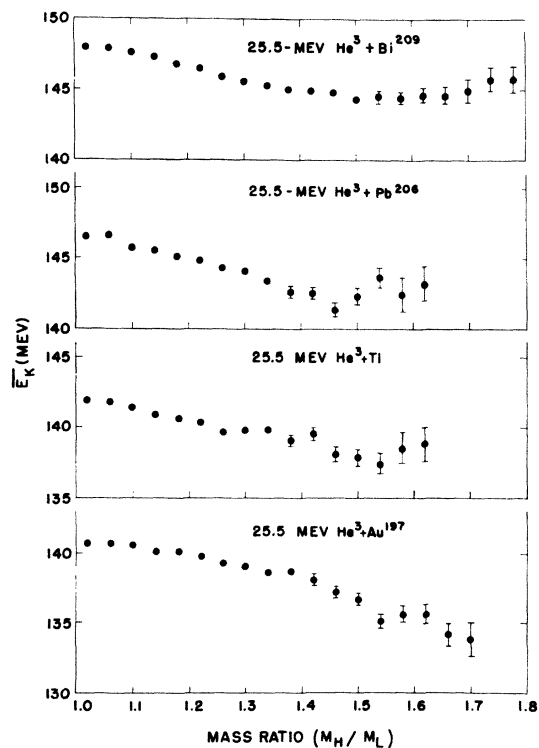FIG. 4. The mass distribution obtained for the 25.5-MeV He[3]-induced fission of Bi[209].

FIG. 6. The average initial total kinetic energy release as a function of the mass ratio of the two fragments for the symmetric fission reactions.

The mass distribution that was obtained for the 25.5-MeV He^3-induced fission of Bi^{209} is shown in Fig. 4. The mass distributions for the other symmetric fission reactions studied are all very similar except for small differences in the widths which will be discussed later. A composite of the mass distributions obtained in the Ra^{226} and Th^{230} reactions is shown in Fig. 5. The mass distributions for the Ra^{226} reactions show the same qualitative features that have been observed by Jensen and Fairhall.[6] The most striking features of the distribution are the strong dependence on excitation energy for the symmetric yield relative to the asymmetric yield, and the large difference in the relative symmetric yield for the He^4 and deuteron reactions at approximately the same excitation energy. It is also interesting to note that the difference in relative symmetric yield between the He^4-induced fission of Ra^{226} and the proton-induced fission of Th^{230} is considerably less than the difference between the He^4- and deuteron-induced fission of Ra^{226}.

The variation of the average initial total kinetic energy release, $\bar{E}_K$, with mass ratio is shown in Fig. 6 for the symmetric fission reactions and in Fig. 7 for the
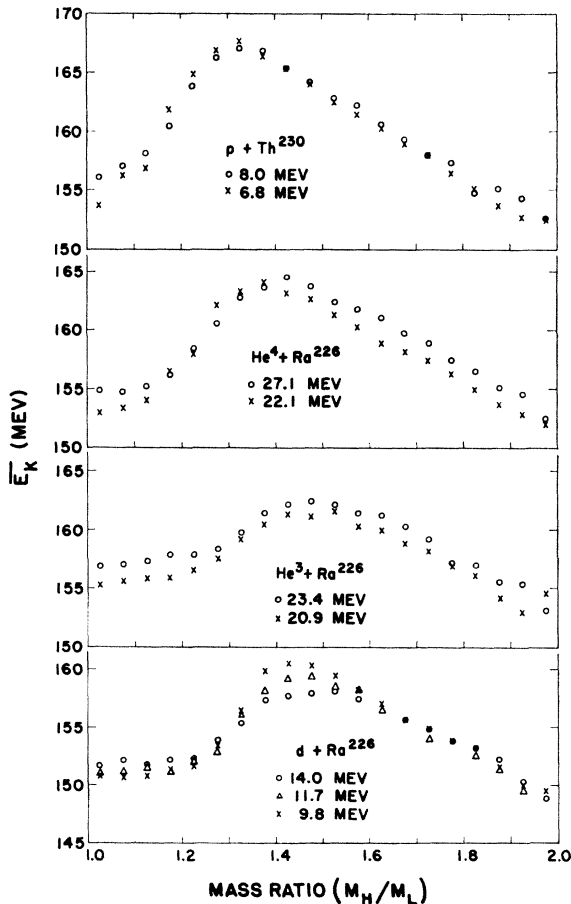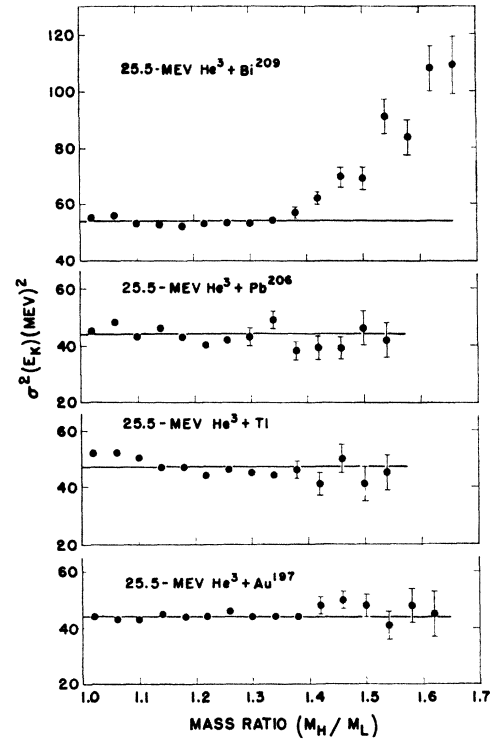
FIG. 8. The variance of the total kinetic energy distributions as a function of the mass ratio of the two fragments for the symmetric fission reactions.

FIG. 7. The average initial total kinetic energy release as a function of the mass ratio of the two fragments for the Ra^{226} and Th^{230} reactions.
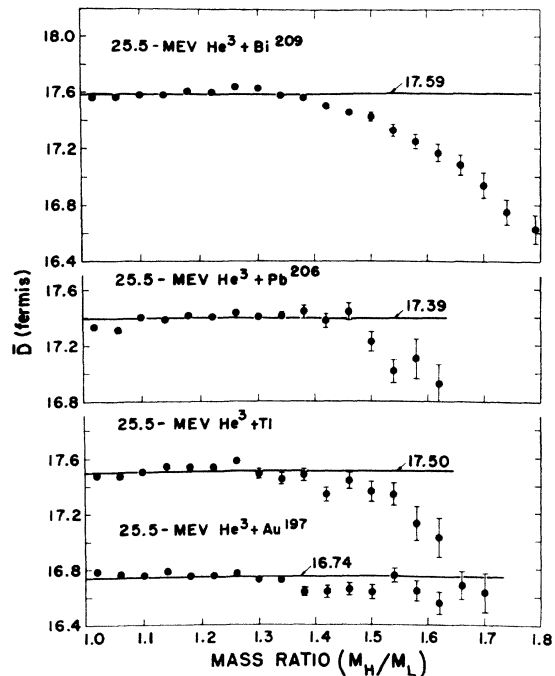
FIG. 9. The average distance between the charge centers of the two fragments at scission as a function of the mass ratio of the two fragments for the symmetric fission reactions.

Ra^{226} and Th^{230} reactions. One significant feature of these results is that the symmetric fission reactions show a maximum for $\bar{E}_K$ at symmetry while all of the other reactions show a decrease in $\bar{E}_K$ in the region of symmetric fission. The dependence of the variance of the total kinetic energy distributions, $\sigma^2(E_K)$, is shown in Fig. 8 for the symmetric fission reactions. These results show that for the mass ratio region 1.0–1.4, which contains >85% of the fragments, $\sigma^2(E_K)$ is independent of the mass ratio. Similarly, for Cf^{252} where only asymmetric fission is present, $\sigma^2(E_K)$ is found to be independent of the mass ratio for mass ratios >1.1 (see Fig. 2). However, for the cases where there is a significant contribution from both symmetric and asymmetric fission, peaks are observed in the $\sigma^2(E_K)$ vs mass ratio curve (see Figs. 10–14). These peaks and the dependence of $\bar{E}_K$ on mass ratio can be interpreted in terms of a competition between two modes of fission with the total kinetic energy release associated with the symmetric fission mode being less than that associated with the asymmetric fission mode. This interpretation is discussed more quantitatively below.

5. ANALYSIS AND DISCUSSION

A. Coulomb Energy Considerations

It was first pointed out by Terrell[26] that the kinetic energy release from fission increased approximately linearly with the Coulomb parameter $Z^2/A^{1/3}$. It has also been shown[1–3] that for a given fissioning nucleus the kinetic energy release is very nearly independent of the excitation energy for the compound nucleus. These results indicate that the total kinetic energy release in fission is probably due primarily to the Coulomb repulsion of the two fragments after scission.

If it is assumed that the kinetic energies of the fragments are due to Coulomb repulsion alone, then the average total kinetic energy release can be written as

$$\bar{E}_K = Z_1 Z_2 e^2/\bar{D}$$

or

$$\bar{D}(\text{fermis}) = 1.439 Z_1 Z_2/\bar{E}_K(\text{MeV})$$

where Z_1 and Z_2 are the nuclear charge numbers for the two fragments. $\bar{D}$ is then the average distance between the charge centers of the two fragments at scission.

Values have been calculated for the average breaking distance, $\bar{D}$, from the $\bar{E}_K$ values shown in Figs. 6 and 7. In computing these values for $\bar{D}$, values for Z_1 and Z_2 from the calculations of Milton[21] were used for the average fragment charges corresponding to the maximum total energy release. The values which are obtained for $\bar{D}$ are dependent on the charge distribution that is assumed for the fragments. The charge distribution used gives essentially the same results as assuming the "equal charge displacement" hypothesis that is commonly used.[1] If the charge ratio is assumed to be the same as the mass ratio, the values for $\bar{D}$ at large

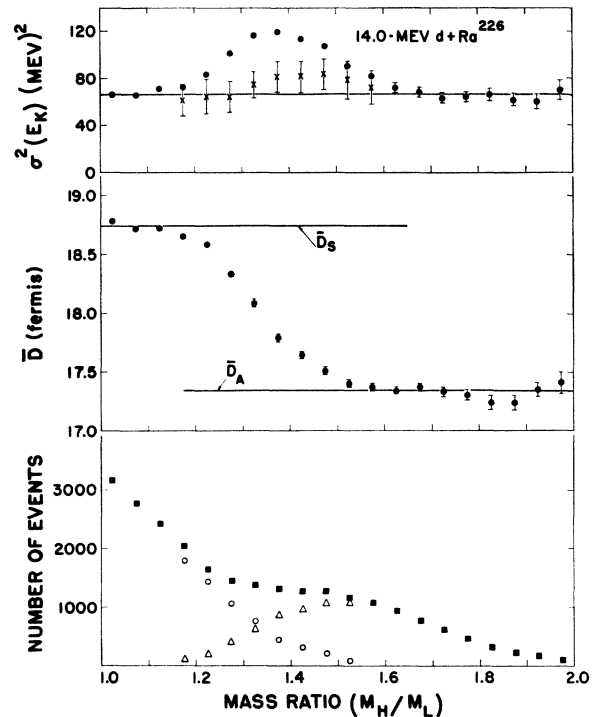^{26} J. Terrell, Phys. Rev. **113**, 527 (1959).

FIG. 10. The yield, $\bar{D}$, and the variance of the total kinetic energy distributions as functions of the mass ratio of the fragments from the 14.0-MeV deuteron-induced fission of Ra^{226}. In the yield distribution the solid squares represent the measured values, and the open circles and triangles are the values determined for the yield from the symmetric and asymmetric modes, respectively. In the $\sigma^2(E_K)$ distribution the solid circles represent the measured values, and $\times$ represents corrected values for $\sigma_i^2(E_K)$ as described in the text.

mass ratios are slightly decreased. For the cases studied the magnitude of this effect corresponds approximately to a 2% change in $\bar{D}$ at a mass ratio of 2.0. Therefore, the major effect of the uncertainty in the charge distribution is to produce a small uncertainty in the slope of the dependence of $\bar{D}$ on the fragment mass ratio.

The dependence of $\bar{D}$ on the mass ratio of the fragments is shown in Fig. 9 for the symmetric fission reactions and in Figs. 10–14 for the heavier element reactions. The results in Fig. 9 show that for the reactions where only the symmetric fission mode is present the distance between the fragment charge centers at scission is constant for mass ratios in the region 1.0–1.4. This mass ratio region contains >85% of the events for the He^3-induced fission of Au^{197} and >95% of the events for the other symmetric fission reactions. Similarly, the Ra^{226} results (see Figs. 10–12) show that for mass ratios greater than 1.5, where only asymmetric mode fission is present, $\bar{D}$ is also independent of the fragment mass ratio.

However, as the fissioning nuclei become heavier, the values obtained for $\bar{D}$ for asymmetric mode fission begin to show a variation with fragment mass ratio. The results from the proton-induced fission of Th^{230} (see Fig. 13) show that for mass ratios greater than 1.4 the

breaking distance $\bar{D}$ increases slightly with increasing fragment mass ratio. The results from the He[4]-induced fission of U[233] show a more rapid increase in $\bar{D}$ with increasing mass ratio in the region 1.4–1.7 and then a subsequent decrease in $\bar{D}$ as the mass ratio increases from 1.7 to 2.0. However, for both of these reactions the values obtained for $\bar{D}$ in the mass ratio range 1.4–2.0 only vary from the average value in that range by approximately $\pm 1\%$.

B. Quantitative Investigation of the "Two-Mode Hypothesis"

In Sec. 4 the "two-mode hypothesis" was shown to give a reasonable explanation for the qualitative features of the results. In this section it is shown that with one reasonable assumption the results obtained for the fission of Ra[226] and heavier elements can be quantitatively explained in terms of a competition between two distinct fission modes.

The basic assumption made for the treatment of the Ra[226] results is that for each fission mode the value for $\bar{D}$ is a constant independent of the fragment mass ratio. This assumption is seen to be reasonable for the sym-
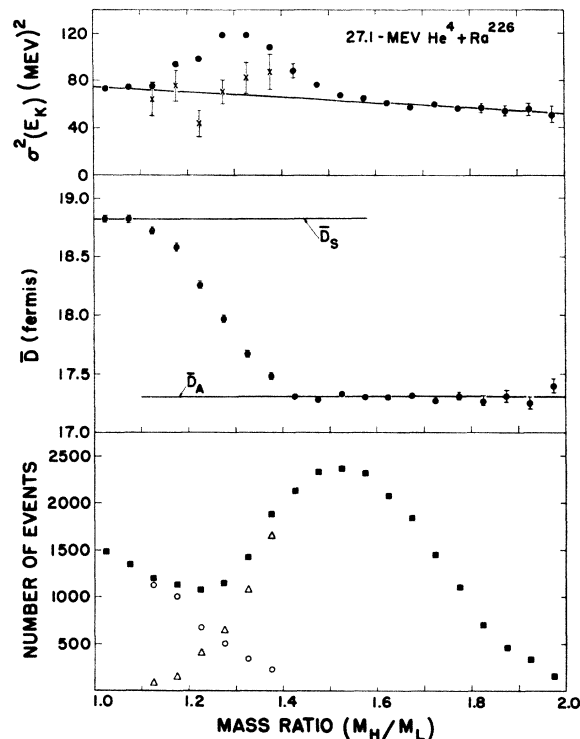

FIG. 11. The yield, $\bar{D}$, and the variance of the total kinetic energy distributions as functions of the mass ratio of the fragments from the 27.1-MeV He[4]-induced fission of Ra[226]. In the yield distribution the solid squares represent the measured values, and the open circles and triangles are the values determined for the yield from the symmetric and asymmetric modes, respectively. In the $\sigma^2(E_K)$ distribution the solid circles represent the measured values, and $\times$ represents corrected values for $\sigma_i^2(E_K)$ as described in the text.
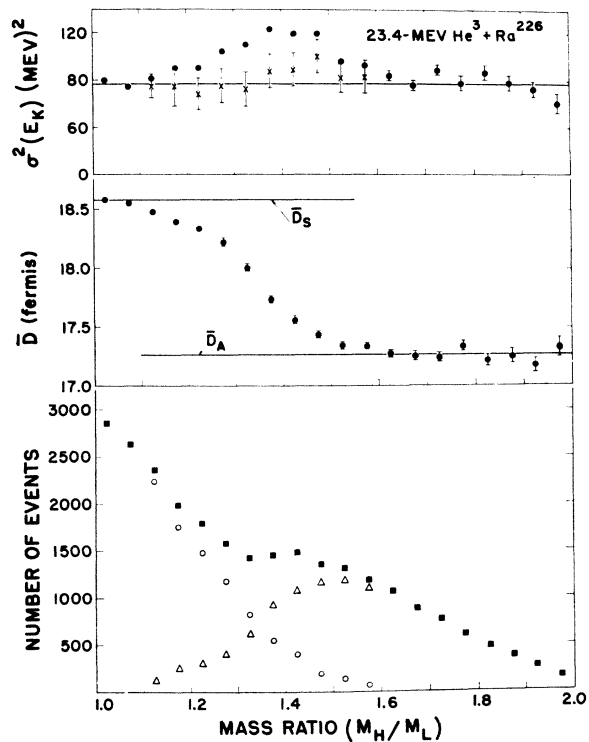

FIG. 12. The yield, $\bar{D}$, and the variance of the total kinetic energy distributions as functions of the mass ratio of the fragments from the 23.4-MeV He[3]-induced fission of Ra[226]. In the yield distribution the solid squares represent the measured values, and the open circles and triangles are the values determined for the yield from the symmetric and asymmetric modes, respectively. In the $\sigma^2(E_K)$ distribution the solid circles represent the measured values, and $\times$ represents corrected values for $\sigma_i^2(E_K)$ as described in the text.

metric fission mode from the results shown in Fig. 9 and for the asymmetric fission mode from the Ra[226] results in Figs. 10–12. The value for $\bar{D}$ for the symmetric mode is then determined from the values obtained at small mass ratios and for the asymmetric mode from the values obtained at large mass ratios as is indicated in Figs. 10–12. Then in the intermediate mass ratio region ($R = 1.1$–1.4) the relative contributions from the two modes can be determined by assuming that the measured value of $\bar{D}$ is simply a weighted average of the values for the two modes, $\bar{D}_A$ and $\bar{D}_S$.

With this two-mode assumption, the measured value of $\sigma^2(E_K)$ in the transition region is then a combination of the intrinsic $\sigma_i^2(E_K)$ for the two modes and an effect due to the difference in the average kinetic energy release for the two modes. If it is assumed that the E_K distributions for a given mass ratio for each mode have a Gaussian shape and that they have the same values for $\sigma_i^2(E_K)$,[27] then the contribution to the measured values $\sigma^2(E_K)$ because of the separation between the

[27] In the regions where only the symmetric or the asymmetric modes contribute, the E_K distributions are approximately Gaussian in shape and $\sigma^2(E_K)$ is approximately the same for the two modes.
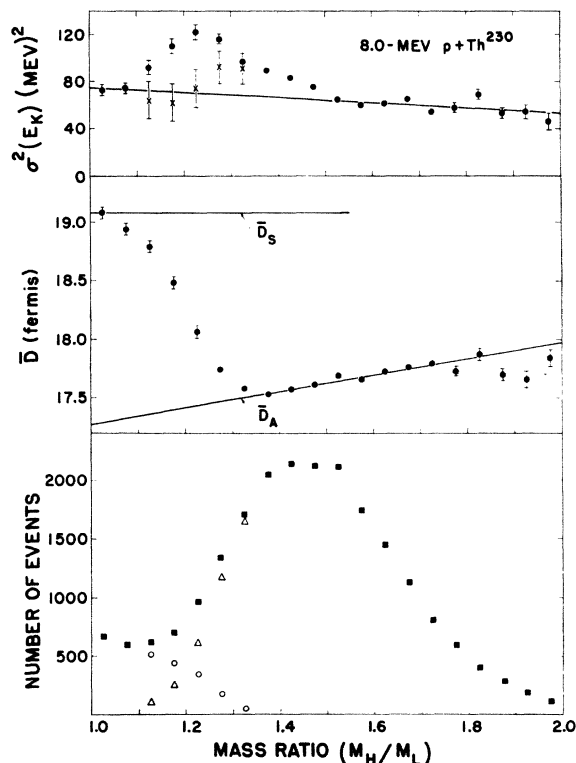
FIG. 13. The yield, $\bar{D}$, and the variance of the total kinetic energy distributions as functions of the mass ratio of the fragments from the 8.0-MeV proton-induced fission of Th[230]. In the yield distribution the solid squares represent the measured values, and the open circles and triangles are the values determined for the yield from the symmetric and asymmetric modes, respectively. In the $\sigma^2(E_K)$ distribution the solid circles represent the measured values, and $\times$ represents corrected values for $\sigma_i{}^2(E_K)$ as described in the text.

two distributions is given by

$$\sigma^2(E_K) - \sigma_i{}^2(E_K) = F(1-F)(\bar{E}_K{}^a - \bar{E}_K{}^s)^2,$$

where F is the fraction of fissions due to the symmetric mode and $\bar{E}_K{}^s$ and $\bar{E}_K{}^a$ are the average total kinetic energy releases for the symmetric and asymmetric modes, respectively.

A test of this two-mode treatment is whether or not this analysis yields values for $\sigma_i{}^2(E_K)$ that vary smoothly with mass ratio, as is observed in the He[3]+Au[197] and the spontaneous Cf[252] fission results in which there is essentially only one mode present. For each of the Ra[226] reactions, an analysis of the type discussed above has been performed. The results of this analysis are shown in Figs. 10–12 for the highest energy case for each reaction. In the reactions where lower bombarding energies were investigated, the results were similar.

It can be seen that for the Ra[226] fission reactions, the analysis yields very reasonable results. In the two reactions where symmetric fission is dominant (deuteron- and He[3]-induced fission of Ra[226]), the values for $\sigma_i{}^2(E_K)$ are independent of mass ratio within the uncertainties

for the points. For the cases where asymmetric fission is dominant (He[4]-induced fission of Ra[226] and proton-induced fission of Th[230]), the corrections for $\sigma^2(E_K)$ are at mass ratios that are low, yielding values for the $\sigma_i{}^2(E_K)$ which are low at the beginning of the transition region and high at the end. However, this effect is small and may be due to the neglect of mass resolution effects or to differences between the values of $\sigma_i{}^2(E_K)$ for the two modes.

The method of analysis described above is not as straightforward for the results from the proton-induced fission of Th[230] and the He[4]-induced fission of U[233] because the assumption that $\bar{D}_A$ is independent of the fragment mass ratio is not valid. In these cases, it was assumed that $\bar{D}_A$ increased linearly with increasing mass ratio as is shown in Figs. 13 and 14. Due to the lack of any information to the contrary, it was assumed that $\bar{D}_S$ was independent of mass ratio. In the case of the proton-induced fission of Th[230], the results obtained from this analysis are reasonable as is shown in Fig. 13. For the He[4]-induced fission of U[233] another difficulty arises because the peak of the asymmetric mass ratio distribution is at a smaller mass ratio than for the Ra[226] reactions so that there may be contributions from the asymmetric
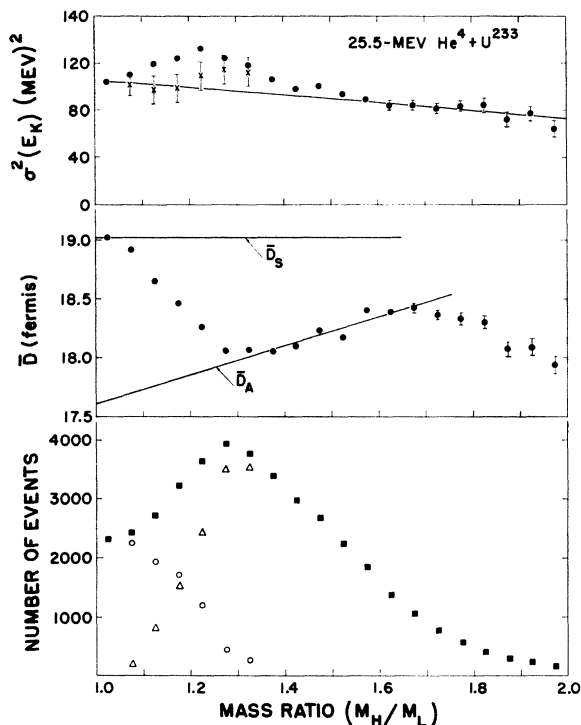

FIG. 14. The yield, $\bar{D}$, and the variance of the total kinetic energy distributions as functions of the mass ratio of the fragments from the 25.5-MeV He[4]-induced fission of U[233]. In the yield distribution the solid squares represent the measured values, and the open circles and triangles are the values determined for the yield from the symmetric and asymmetric modes, respectively. In the $\sigma^2(E_K)$ distribution the solid circles represent the measured values, and $\times$ represents corrected values for $\sigma_i{}^2(E_K)$ as described in the text.
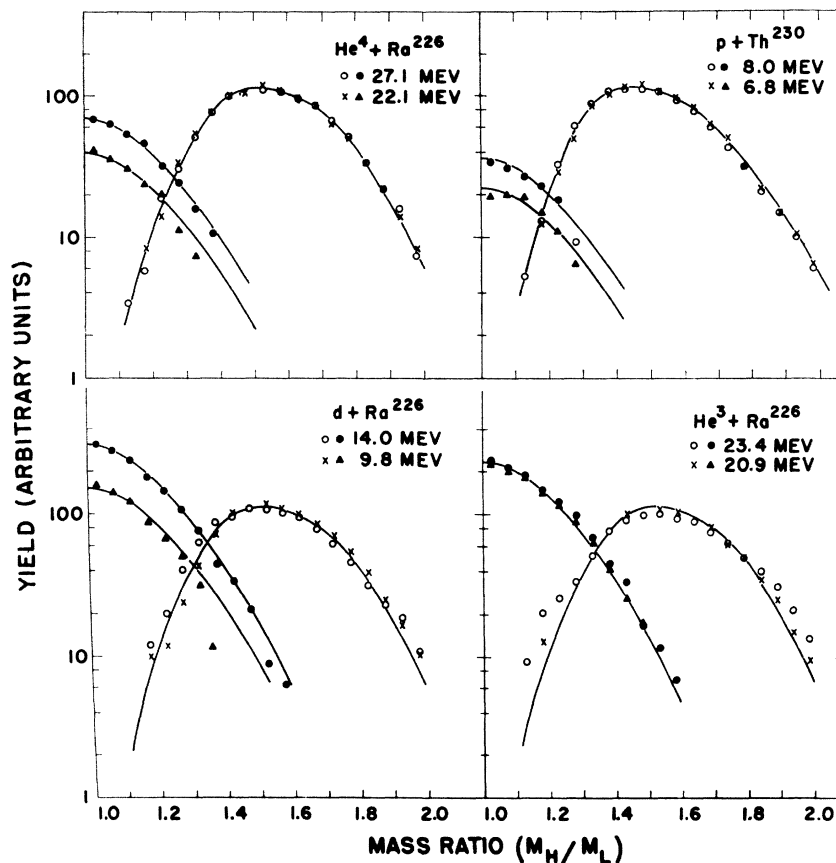
FIG. 15. The mass ratio distribubutions for the symmetric and asymmetric modes from several of the reactions studied.

mode at symmetry ($R=1.0$). This results in a large uncertainty in the value for $\bar{D}_S$ which yields a corresponding uncertainty in the relative symmetric yield. However, the results shown in Fig. 14 are qualitatively reasonable and indicate the presence of contributions from the two modes.

The yields that are obtained from this analysis of the symmetric and asymmetric modes are summarized in Fig. 15 for all of the reactions studied. The distributions shown in Fig. 15 have been normalized to make the area of the asymmetric distribution the same for all of the reactions. The solid-line fits to the symmetric mode distributions were obtained from the best fit by eye to the 14.0-MeV $d+\mathrm{Ra}^{226}$ results where the symmetric mode is predominant. This distribution was then arbitrarily normalized to obtain the best fit to the symmetric mode distributions obtained for the other reactions. Figure 15 indicates that the yield distributions for the symmetric mode all have approximately the same shape. In a similar manner the solid line fits to the asymmetric yield distributions for the Ra^{226} reactions were obtained from a fit to the 27.1-MeV He$^4+$Ra^{226} results where the asymmetric mode is predominant. The results show that the yield distributions for the asymmetric mode also have approximately the same shape for all of the Ra^{226} cases. For the Th^{230} reactions the peak of the asymmetric distribution is at a smaller mass

ratio in agreement with the trend for heavy fissioning nuclei.[1-3] The fit to the symmetric distribution is also shown in Fig. 16, in comparison to the mass ratio distributions for the symmetric fission reactions. It can be seen that the shape is similar to the distribution for the 25.5-MeV He^3-induced fission of Bi^{209}.

In addition to the above analysis of the fragment mass ratio distributions, the mass distributions for the Ra^{226} and Th^{230} reactions have been fitted by a least-squares method assuming that they consist of a sum of three Gaussian peaks. The results of this analysis are summarized in Table I. This analysis gives relative yields for the two modes that are approximately the same as the values obtained from the above analysis of the mass ratio distributions.

In the Ra^{226} and heavier element reactions the yield for the symmetric component varies from 10 to 60% of the total yield. Since this method of analysis yields mass ratio distributions for the two modes that have the same shapes over this large range, the validity of the two-mode hypothesis is strongly indicated.

In analogy to the Ra^{226} results, the decrease in $\bar{D}$ at large mass ratios and the corresponding increase in $\sigma^2(E_K)$ (see Figs. 8 and 9) may be evidence for the presence of a small asymmetric component in the 25.5-MeV He^3-induced fission of Bi^{209}. This component would be in approximately the same mass region as the
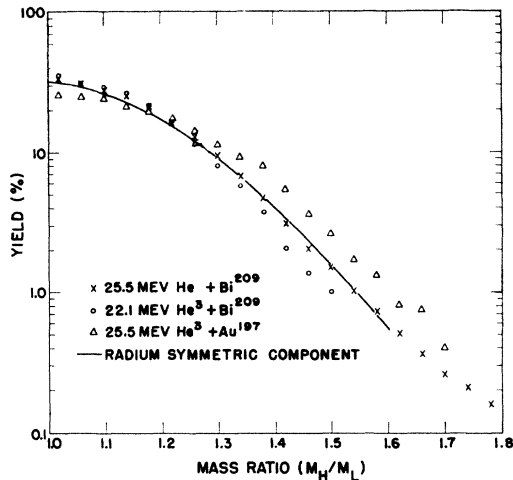
FIG. 16. The mass ratio distributions from the symmetric fission reactions and for the symmetric mode in the Ra^{226} reactions.

asymmetric component observed by Sugihara et al.[28] in the proton-induced fission of Bi^{209}, and would have about the same intensity ($\sim 1\%$ of the total fissions). With the mass resolution of these measurements, it would not be possible in the mass distribution to resolve a low intensity narrow asymmetric component such as was observed by Sugihara et al.,[28] and indeed the observed mass distribution (see Fig. 4) does not show any indication for an asymmetric component except for a possible change in slope at large mass ratios in the mass ratio distribution shown in Fig. 16. If this interpretation for the energetics is correct, these results indicate that the variation in $\bar{D}$ and $\sigma^2(E_K)$ distributions are a very sensitive method for detecting small contributions from the asymmetric or symmetric modes.

C. Fission Systematics

From the results presented above, it is possible to obtain quantitative information on the variation of several of the parameters that are of interest in the study of the fission process. The information that can be obtained is: the variation of the relative symmetric yield with both E^* and Z^2/A; the variation of the average breaking distance, $\bar{D}$; and the variation in the widths of the mass distributions as a function of both E^* and the mass of the fissioning nucleus for the symmetric fission reactions.

The relative symmetric yields for the reactions studied are plotted in Fig. 17. These results show a very strong dependence for the change in the symmetric yield from the deuteron-induced fission of Ra^{226} to the He^4-induced fission of Ra^{226}. This change is more striking when compared to the smaller changes observed between the He^4-induced fission of Ra^{226} and the other fission reactions. Unfortunately, the interpretation of these results is not at all clear because of the possible con-

tributions from second-chance fission. Huizenga[29] has pointed out that fission cross section and angular distribution measurements for the He^4-induced fission of Ra^{226} indicate a significant contribution from second-chance fission after evaporation of a neutron. The contribution from second-chance fission is probably much less for the deuteron-induced fission of Ra^{226} for which the fission cross sections are much smaller, and increase more rapidly with excitation energy. This would mean that an appreciable contribution from second-chance fission in the He^4- and He^3-induced fission of Ra^{226}, and the He^4-induced fission of U^{233}, would tend to decrease the relative symmetric yield compared to the relative symmetric yield for first-chance fission. The proton-induced fission of Th^{230} is probably all first-chance fission because the excitation energies are below or very near the second-chance fission threshold. A second-chance fission contribution in the He^4-induced fission of Ra^{226} would explain why the symmetric yields from the proton-induced fission of Th^{230} and the He^4-induced fission of Ra^{226} are comparable even though the proton reaction has a higher Z^2/A and a lower excitation energy. These second-chance fission effects would tend to make the relative symmetric yields for first-chance fission in the radium region decrease less rapidly than might be concluded from the results in Fig. 17. This would also account for the fact that energy dependence is not as strong for the He^3- and He^4-induced fission of Ra^{226} as for the deuteron-induced fission of Ra^{226} and proton-induced fission of Th^{230}.

The results that have been obtained for the widths of the mass distributions for the symmetric fission reactions are given in Table I. The values of the variance of the symmetric mass distributions, $\sigma_s^2(m)$, have been corrected for the dispersion due to electronic noise discussed in Sec. 2, but no corrections have been made for the dispersion due to neutron emission effects discussed in Sec. 3C. There are two general trends in the results. The values of σ^2 tend to increase as the mass of the compound nucleus decreases and the widths increase with increasing excitation energy. These effects are both
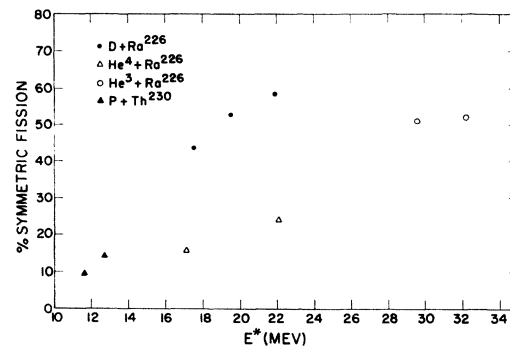

FIG. 17. The relative symmetric yield as a function of the excitation energy of the compound nucleus for the reactions studied.

[28] T. T. Sugihara, J. Roesmer, and J. W. Meadows, Phys. Rev. 121, 1179 (1961).

[29] J. R. Huizenga (private communication); J. E. Grindler, G. L. Bate, and J. R. Huizenga, Bull. Am. Phys. Soc. 7, 303 (1962).

consistent with the trend that has been pointed out by Terrell;[22] the symmetric mass distributions seem to be constricted to the region where the heavy fragment has a charge less than the closed shell of 50 protons, and as the excitation energy is increased, this constriction seems to become less important. For the mass distributions from the heavier fissioning nuclei, it is found that in all cases the division between dominant symmetric mode fission and dominant asymmetric mode fission occurs at approximately the point where the heavy fragment contains the closed shell of 50 protons. This general trend in fission mass distribution has also been pointed out by Terrell.[22]

The values which have been obtained for $\bar{D}_A$ and $\bar{D}_S$ from the analysis described in Sec. 5B are plotted in Fig. 18. For the Th^{230} and U^{233} reactions, where $\bar{D}_A$ was found to vary with the fragment mass ratio, the values of $\bar{D}_A$ for the most probable asymmetric fragment mass ratio have been plotted. The results in Fig. 18 again show that the average breaking distance for a given fissioning nucleus is greater for the symmetric than for the asymmetric mode. These results also show that for a given mode $\bar{D}$ increases with increasing mass of the fissioning nucleus and that the rate of increase is approximately the same for each mode.

A general trend that can be seen in the results in Figs. 7 and 18 is that, for all cases where more than one bombarding energy was investigated for a given reaction, the $\bar{E}_K$ values are slightly lower for the lower energy reaction. This decrease in $\bar{E}_K$ is approximately 0.1% per 1-MeV change in the bombarding energies. These changes are extremely small, and are just about equal to the limit estimated for the stability of the electronic equipment used. However, the fact that these changes in $\bar{E}_K$ with bombarding energy were in the same direction and about the same magnitude for all cases indicates that they are probably real. This effect may well be experimental, but at present no reason can be seen for it.[30] If this effect is real, it may be an indication that the fragments possess a small amount of kinetic energy at the scission point or, conversely, that the scission shapes become less distorted as the excitation energy is increased. In either case, the effect is very small, and it is probably more remarkable that the results are so nearly independent of the excitation energy of the compound nucleus.

If the measurements of the thermal neutron-induced fission of U^{233}, U^{235}, and Pu^{239}, which have been reported by Milton and Fraser,[8] are analyzed in the manner described in Sec. 5A, the results are somewhat different from the results obtained for the reactions investigated in this experiment. First, the values obtained for $\bar{D}_A$ increase more rapidly with increasing mass ratio than the values obtained from He^4-induced fission of U^{233}. In
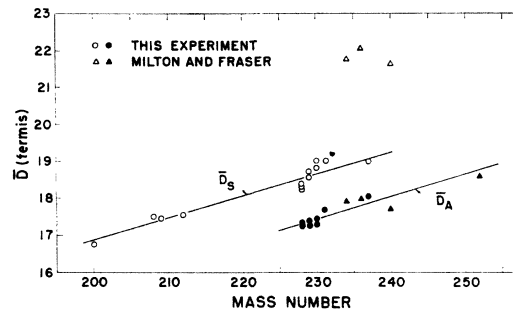

FIG. 18. The variation of $\bar{D}$ as a function of the atomic number, A, of the fissioning nucleus. The closed points are results of this experiment, and the open points are taken from measurements of Milton and Fraser (see reference 8) for thermal-neutron-induced fission reactions. The multiple points appearing at some A values represent data taken at different bombarding energies. In all cases, the lower bombarding energies correspond to higher $\bar{D}$ values.

order to compare with the results of this experiment, values for $\bar{D}_A$ and $\bar{D}_S$ from the thermal neutron measurements have been plotted in Fig. 18. The values of $\bar{D}_A$ correspond to the values for the most probable mass division. The values of $\bar{D}_S$ were taken from the total kinetic energy release for a symmetric mass division ($R=1.0$). Figure 18 shows that the values obtained for $\bar{D}_A$ agree quite well but that the $\bar{D}_S$ values are greater for the thermal neutron results than for the results of the present experiment. Similar results have been obtained for the thermal neutron-induced fission of U^{235} from measurements of the fragment energies[9] and ranges.[10] However, in all of these cases a symmetric mass division is extremely improbable and, therefore, very difficult to observe experimentally, so that the $\bar{D}_S$ values shown in Fig. 18 for the thermal neutron results may be subject to rather large uncertainties.[31] Therefore, it is not clear whether a difference really exists between these thermal neutron results and the results of this experiment. It is also not clear whether the two-mode explanation that has been applied to these charged particle results is applicable to the thermal neutron results.

6. SUMMARY

The results obtained from this experiment point out several interesting properties of the fission process. First, these results for the fission of compound nuclei with moderate excitation energies are quantitatively consistent with the hypothesis that the fission proceeds via two distinct modes, a symmetric fission mode and an asymmetric fission mode. With this two-mode explanation, the results then show that the total kinetic energy release is greater for asymmetric mode than for symmetric mode fission. If it is assumed that the total kinetic energy release arises from the Coulomb repulsion of the fragments, then these results indicate that the average distance between charge centers at scission is greater for symmetric mode fission.

---

[30] The observed decreases in K are about a factor of 10 too large to be accounted for either by center-of-mass effects which have been neglected or by effects due to second-chance fission competition.

[31] J. C. D. Milton (private communication).

A detailed analysis of the results indicates that for the compound nuclei formed in the Ra^{226} and lighter element reactions this average breaking distance is independent of the fragment mass ratio for a given mode. However, for the heavier compound nuclei, Pu^{231} and Pu^{237}, these measurements indicate that the average breaking distance for asymmetric mode fission increases slightly with increasing mass ratio. The magnitude of this variation with mass ratio is less than is obtained from measurements[8–10] of the total kinetic energy releases for thermal neutron-induced fission reactions. These differences indicate that the dependence of the average breaking distance on the fragment mass ratio is probably a function of both the mass or Z^2/A and the excitation energy of the compound nucleus.

However, the results indicate that at least for asymmetric mode fission the average breaking distance is only very slightly dependent on the excitation energy of the compound nucleus. For the symmetric mode the average breaking distances are found to be approximately independent of the excitation energy at moderate excitations but may be somewhat different for the lower excitation energy thermal neutron-induced fission.

For both modes the average breaking distance is found to increase as the mass of the compound nucleus increases.

Elastic Scattering of Alpha Particles from Helium*

T. A. TOMBRELLO AND L. S. SENHOUSE

California Institute of Technology, Pasadena, California

(Received 1 October 1962)

The scattering of alpha particles from He^4 has been studied for laboratory energies between 3.8 and 12 MeV. Ten angular distributions have been measured over this range of energies as well as excitation curves at the center-of-mass angles 30.6°, 40°, 54.8°, 70.2°, and 90°. A phase-shift analysis of these data has been made and is compared to previously published results.

INTRODUCTION

EXPERIMENTAL investigation of the scattering of alpha particles from He^4 was first made by Rutherford and Chadwick[1] using alpha particles from natural sources. Further measurements by Chadwick[2] and by Blackett and Champion[3] showed that the scattering exhibited the strong deviations from classical Coulomb scattering that had been predicted by Mott.[4]

In recent years, the availability of intense alpha-particle beams from accelerators and the development of improved detection techniques have allowed precise experimental data to be taken for bombarding energies between 150 keV and 38.4 MeV.[5–9] Our purposes in seeking to add to this rather extensive body of data were to cover the previously untouched energy region between 9 and 12 MeV and to resolve certain small disagreements between published results near 7 MeV.[7,10,11] These disagreements, though small in themselves, are

* Supported in part by the Joint Program of the Office of Naval Research and the U. S. Atomic Energy Commission.
[1] E. Rutherford and J. Chadwick, Phil. Mag. 4, 605 (1927).
[2] J. Chadwick, Proc. Roy. Soc. (London) A128, 120 (1930).
[3] P. M. S. Blackett and F. C. Champion, Proc. Roy. Soc. (London) A130, 380 (1931).
[4] N. F. Mott, Proc. Roy. Soc. (London) A126, 259 (1930). A summary of early experimental work is given by J. A. Wheeler, Phys. Rev. 59, 16 (1941).

[5] E_α=0.15 to 3 MeV: N. P. Heydenburg and G. M. Temmer, Phys. Rev. 104, 123 (1956).
[6] E_α=2.5 to 5.5 MeV: J. L. Russell, G. C. Phillips, and C. W. Reich, Phys. Rev. 104, 135 (1956).
[7] E_α=5.0 to 9 MeV: C. M. Jones, G. C. Phillips, and P. D. Miller, Phys. Rev. 117, 525 (1960).
[8] E_α=12 to 23 MeV: R. Nilson, R. O. Kerman, G. R. Briggs, and W. K. Jentschke, Phys. Rev. 104, 1673 (1956); R. Nilson, W. K. Jentschke, G. R. Briggs, R. O. Kerman, and J. N. Snyder, ibid. 109, 850 (1958).
[9] E_α=23 to 38.4 MeV: D. J. Bredin, W. E. Burcham, D. Evans, W. M. Gibson, J. S. C. McKee, D. J. Prowse, J. Rotblat, and J. N. Snyder, Proc. Roy. Soc. (London) A251, 143 (1959).
[10] N. Berk, F. E. Steigert, and G. L. Salinger, Phys. Rev. 117, 531 (1960).
[11] J. R. Dunning, A. M. Smith, and F. E. Steigert, Phys. Rev. 121, 580 (1961).